# Conceptual Design of Distillation Processes for Mixtures with Distillation Boundaries: I. Computational Assessment of Split Feasibility

**Stefan Brüggemann**
BASF SE, Verbund Structures Europe, D-67056 Ludwigshafen, Germany

**Wolfgang Marquardt**
Lehrstuhl für Prozesstechnik, RWTH Aachen, Turmstraβe 46, D-52056 Aachen, Germany

*DOI 10.1002/aic.12378*
*Published online August 23, 2010 in Wiley Online Library (wileyonlinelibrary.com).*

*Geometric design methods for the conceptual design of azeotropic distillation processes are fast and efficient tools for the economic screening of different process alternatives. This two-part series presents a fully automated conceptual design method for finding an optimal recycle policy for the separation of mixtures with distillation boundaries. It does not require visualization and graphical inspection of residue curve or pinch maps and is, hence, not limited to ternary mixtures. The first part introduces a fully computational geometric split feasibility test based on bifurcation analysis. This bifurcation-based feasibility test can be used as a valuable stand-alone tool for the assessment of different separation options. It is also one of the core elements of the recycle optimization discussed in the second part of this series.* © 2010 American Institute of Chemical Engineers *AIChE J,* 57: 1526–1539, 2011
*Keywords: design (process simulation), distillation, mathematical modeling, process synthesis, simulation, process*

## Introduction

The design of a separation process for azeotropic mixtures frequently gives rise to a large number of different process configurations. Each of these processes is itself characterized by several internal degrees of freedom arising from recycle loops within the process. The high level of complexity both with respect to structural and internal degrees of freedom renders the design of such separations a demanding task. In industrial practice, the design problem is usually addressed by means of extensive simulation studies. However, due to the time-demanding nature of this approach, only a small selection of promising process alternatives and internal degrees of freedom is analyzed, whereas other potentially attractive alternatives are discarded.

In recent years, geometric design methods for the conceptual design of azeotropic distillation processes have become an established and valuable addition to purely simulation-based design.[1] On a qualitative level, the analysis of azeotropes, miscibility gaps, distillation boundaries, and residue curves enable the identification of typical thermodynamic topologies.[2–6] The topology information contained in the residue curve map can be used to develop a suitable flow sheet structure including the placement of recycle streams.

Figure 1 illustrates the use of residue curve maps for graphical process design for a ternary mixture with a strongly curved distillation boundary (example taken from Stichlmair and Fair[7]). The purification of ethanol from the dilute aqueous feedstock F with the concentration $\mathbf{x}_F$ is desired. Tetrahydrofurane (THF) is used as an entrainer. To

Correspondence concerning this article should be addressed to W. Marquardt at wolfgang.marquardt@avt.rwth-aachen.de.

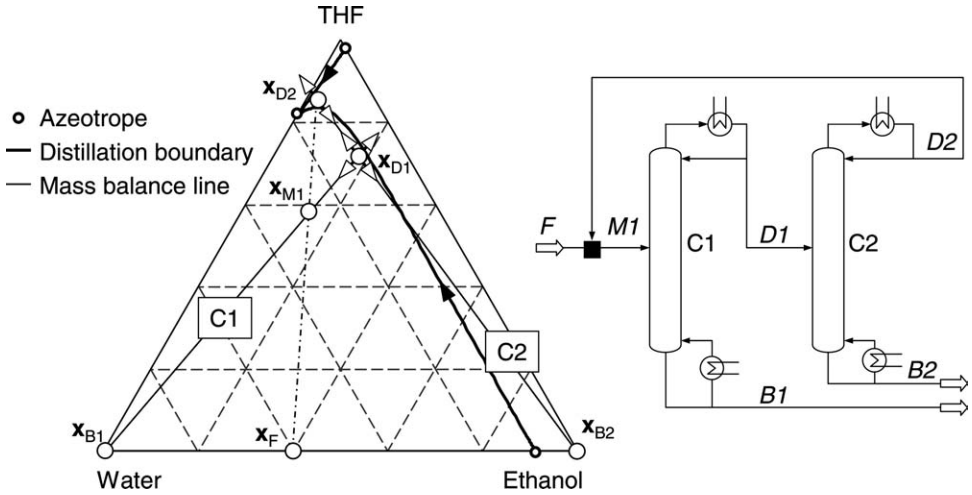


**Figure 1. Two-column process for the purification of ethanol by exploitation of a highly curved distillation boundary.**

produce high-purity ethanol, the distillation boundary between the ethanol–water and the THF–water edges must be crossed without violating the rule for feasible product specifications in a distillation column, i.e., the compositions of the distillate and the bottoms product must lie on the same side of the distillation boundary. The boundary crossing is achieved in column C2 that produces high-purity ethanol at the bottom and a concentration close to the binary THF–water azeotrope at the top. The distillate *D2* is an undesired cut, which is recycled and mixed to the feed *F*. The resulting stream *M1* is fed to column C1, where water is removed in the bottom product *B1*. Hence, the complete separation of the feed mixture is achieved by a clever combination of mixing and separating and the exploitation of the curvature of the boundary.

For ternary mixtures, it is often not necessary to design such processes from scratch. Manan et al.[8] assign a catalog of distillation sequences to certain classes of topology. Stichlmair and Herguijuela[9] recommend standardized distillation processes for some ternary topologies and show the application to several industrially significant example mixtures. Further examples as well as detailed explanations on the design of distillation processes based on topology information can be found in the textbooks of Doherty and Malone[10] and Stichlmair and Fair[7] and the references given therein. In all cases, the graphical design approach is based on the knowledge of the distillation boundaries with respect to their location, curvature, and pressure sensitivity. Furthermore, the idea of design based on thermodynamic analysis can be extended beyond homogeneous distillation. For example, liquid–liquid phase splitting[11,12] and limitation by chemical reaction equilibrium[13] can be integrated. The concept can even be transferred to melt crystallization by replacing vapor–liquid equilibrium with solid–liquid equilibrium.[14]

Geometric design methods can also be used for an economic evaluation of the different alternative process configurations. In this case, the visual inspection of the distillation boundaries is coupled with a suitable performance calculation of each column. Frequently, minimum reflux algorithms are used to provide this performance calculation. The minimum reflux ratio corresponds to the minimum energy demand of the column, which can be used as a coarse measure for the expected operating cost. Roughly, one could say that the minimum energy calculation serves as a targeting method for economical fitness of the column. A large number of geometric shortcut methods are available to provide this targeting. The fully graphical boundary value method[15] is probably the one most widely used in literature for case studies.

The major limitation of the graphical design approach, both with respect to checking split feasibility and assessing column performance, is its dependency of a useful visualization of the thermodynamical properties of the mixture in a diagram. Generally, this property limits the approach to ternary mixtures. The application to more complex mixtures by lumping of components,[16] simplification of the boundary geometry,[17,18] or specialized projection techniques[19,20] only succeeds in exceptional cases.

Recent research in this field has focused on retaining the concepts behind graphical design methods based on residue curve maps, while eliminating the need for visual inspection and, hence, the restriction to ternary mixtures. A sequence of articles by Lucia and coworkers[21–24] proposes geometric-based methods with optimization formulations for calculating exact separation boundaries. Among the proposed formulations are the constrained maximization of a line integral for ternary mixtures and a surface area, volume, or hypervolume constrained by the Levi-Civita parallelism for mixtures with four or more components. These formulations are combined with minimum reflux calculation based on the concept of stripping line distance.[25,26] Other authors transform the feasibility check to a numerical temperature collocation.[27]

In this two-part article series, a novel optimization framework for the economic assessment of competing process configurations will be presented. The new approach is fully computational and does not require visualization and graphical inspection. Hence, it can be applied to mixtures of arbitrary complexity. One of the key ingredients of this approach is the formulation of a reliable computational feasibility check for any proposed split. The first part introduces a novel geometric split feasibility test based on bifurcation analysis. The feasibility test determines the distance between

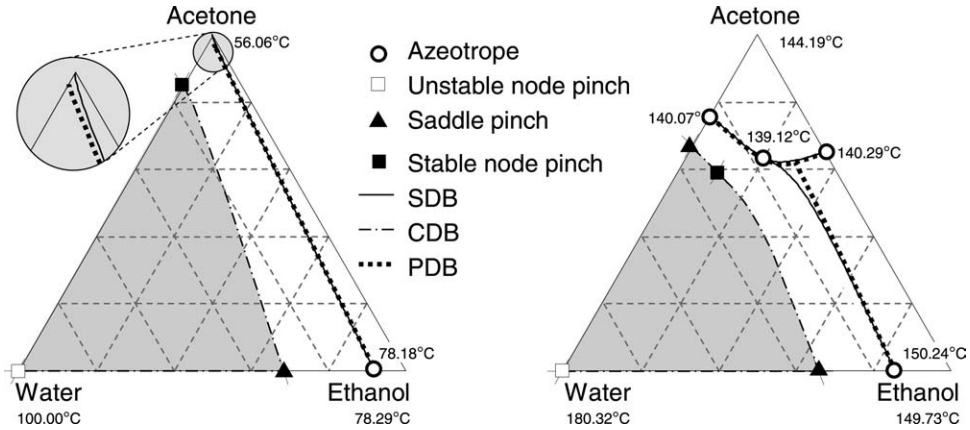


**Figure 2. Comparison of different formulations of the distillation boundaries at pressures of $p = 1$ atm (left) and $p = 10$ atm (right).**

The SDB, the CDB (for the stripping section, production of essentially pure water in the bottom product and a boil-up ratio $s = 10$), and the PDBs are shown. The shaded area highlights the part of the composition space which can be accessed in the stripping section according to the CDB.

the products of the desired split and the distillation boundaries. Hence, it does not only give a yes-or-no assessment but also provides sensitivity information with respect to the location of the product compositions. This property is one of the prerequisites for the incorporation of the feasibility test into the optimization framework presented in the second part of the article series.

## Definitions of Distillation Boundaries

Azeotropic mixtures with saddle azeotropes, i.e., where the azeotrope is an intermediate boiler, are characterized by the appearance of distillation boundaries, which limit the feasible products of a column. In the scientific literature, these boundaries are predominantly determined on the basis of limiting residue curves. Two additional formulations for the boundaries are known. They are based on limiting conditions of tray-by-tray profiles or pinch branches.[10] To lay the theoretical foundations for the discussion of the new bifurcation-based feasibility test, the three different formulations and their computational properties are briefly discussed and screened for their qualification for the use in a computational feasibility test.

### *Simple distillation boundaries*

The conceptual analysis of column behavior is often based on residue curves. These curves describe the course of the composition profile of an open evaporation with respect to time. They are calculated using the set of ordinary differential equations

$$\frac{dx_i}{dt} = x_i - y_i^*(\mathbf{x}, p), \quad i = 1, \ldots, C-1, \tag{1}$$

where $\mathbf{y}^*$ is the vapor composition in equilibrium with the liquid composition $\mathbf{x}$. Alternatively, residue curves can be interpreted as the composition profile along the height of a packed column,[10] whereas the composition profiles of tray columns are called rectification lines[28] and can be calculated from a different set of equations. Usually, the slight difference between residue curves and rectification lines can be neglected. Hence, the conceptual design of a split in a distillation column is usually based on an analysis of the residue curve map regardless of the type of the column internals.

According to Eq. 1, residue curves have the advantageous property that they only depend on the column pressure $p$ and the initial composition $\mathbf{x}$. Consequently, the structure of the residue curve map only depends on the column pressure $p$. The same argumentation applies for limiting residue curves that connect the saddle azeotropes to some other singular points, i.e., other azeotropes or pure component vertices. Using the common assumption that the composition profiles of columns operated at finite reflux are qualitatively identical to the ones at infinite reflux, the limiting residue curves describe the boundary for the product compositions of a simple distillation column. Such distillation boundaries based on the limiting residue curves are named simple distillation boundaries (SDB). Figure 2 shows the SDB for a ternary mixture of acetone, ethanol, and water at two different pressures. The significant pressure-sensitivity of the boundaries can be used for the synthesis of a pressure-swing process as discussed in the second part of this series.

With respect to the synthesis and design of distillation processes, the representation of the boundaries in the composition space as given in Figure 2 can be used for a graphical feasibility check of any desired split. In the case of ternary mixtures, the feasibility check can also be performed computationally.[29] However, both the graphical and the computational evaluation of the SDB can hardly be extended to mixtures with four or more components, where the boundaries form surfaces or multidimensional hypersurfaces. For the graphical evaluation, this limitation is caused by the inability to visualize the composition space. Even with very sophisticated visualization techniques, at most quaternary mixtures may be considered with great difficulty.[30]

Computational formulations for the feasibility test frequently fail because there is no suitable closed form function $\mathbf{f}(\mathbf{x}) = \mathbf{0}$ that allows the determination of the composition,

where the mass balance line of the column intersects with the distillation boundary. As a consequence, most state-of-the-art algorithms for checking the feasibility of multicomponent splits use some approximation of the boundaries. Rooks et al.[17] linearly connect all singular points of the residue curve map to obtain a planar representation of the boundaries. This method is robust and computationally efficient. However, the linear approximation of the boundaries frequently leads to large errors and explicitly eliminates potentially attractive process alternatives, which exploit a strongly curved boundary.[31] Recent methods for the approximation of the distillation boundaries use nonlinear hypersurfaces based on spheres, ellipsoids, or polynomials, which are, in principle, able to overcome some of the limitations of the linear surface.[32] However, the need for effective algorithms to determine the intersection of a line and the nonlinear hypersurface and the fitting of the hypersurface to the real boundary adds complexity to the calculation. Bellows and Lucia[23] present successful examples for the application of fitted surfaces for the calculation of separation boundaries of mixtures with four components.

As an alternative to the approximation of the boundaries in high-dimensional space the projection of the split to a planar subsystem[33] or the direct evaluation of a large number of residue curves[34] may be considered. However, these methods are hardly suitable for integration into an automated computational method based on an optimization algorithm. On one hand, the required computational effort is too large. On the other hand, these methods allow to obtain only a yes-or-no assessment of feasibility. They do not characterize the degree of feasibility or infeasibility and, therefore, cannot be used to provide the required gradients of the feasibility evaluation for integration into a mathematical optimization strategy.

### *Continuous distillation boundaries*

Vogelpohl[35] and Nikolaev et al.[36] show that the attainable product compositions in simple columns at finite reflux are, in addition to the column pressure $p$, also dependent on the product specifications $\mathbf{x}_D$ and $\mathbf{x}_B$ and the reflux ratio $r$. The corresponding distillation boundaries are termed continuous distillation boundaries (CDB) by Fidkowski et al.[37] The determination of the CDB can be accomplished by a calculation of the tray-by-tray profiles originating from the saddle pinch points. The respective algorithms and systems of equations can be found in the literature.[38] In analogy to the definition of the limiting residue curves, these special tray-by-tray profiles are termed limiting profiles.

Figure 2 shows the CDB and the region of attainable compositions of the stripping section of a column with a reboil ratio $s = 10$, which produces a high-purity water stream in the bottom product. For industrially relevant reflux or reboil ratios, the limiting tray-by-tray profiles are often qualitatively similar to the limiting residue curves. However, sometimes a CDB intersects the respective SDB.[31] Furthermore, there exists a noteworthy number of mixtures for which the behavior of the tray-by-tray profiles differs from the residue curves not only quantitatively but also qualitatively. Especially, heterogeneous separations often show such behavior.[39]

The use of CDB for the development of a feasibility test, which can be integrated into an optimization algorithm, is impeded by similar arguments as already given above for the SDB. Methods for the calculation of a single point on the boundary as well as for the determination of the gradients describing the change in the degree of feasibility are missing. Even worse, the additional dependency of the profiles with respect to the column section (rectifying or stripping section), product composition, and reflux further complicates the application of the CDB for a feasibility analysis.

### *Pinch distillation boundaries*

Pinch branches correspond to the concentration profile of a reversible separation, i.e., intermediate heaters and coolers along the column supply energy such that in total no energy is emitted to the environment.[40] Hence, a feasible specification of products requires that the distillate product $\mathbf{x}_D$ and the bottom product $\mathbf{x}_B$ are connected by a continuous path of pinch branches. Figure 3 shows the pinch branches of the rectifying section for three different specifications of $\mathbf{x}_D$ at $p = 1$ atm. For $x_{D,water} < z_{water}$ in Figure 3a, a pinch branch connects $\mathbf{x}_D$ with the pure ethanol vertex. A reversible column can, therefore, produce high-purity ethanol. A second pinch branch runs between the azeotrope and the pure water vertex. As there is no connection between this second pinch branch and $\mathbf{x}_D$, the respective compositions cannot be reached in a reversible column. Such pinch branches are termed "disjunct pinch branch".

Figure 3b shows the pinch map for $x_{D,water} > z_{water}$, i.e., a distillate composition slightly richer in water. In this case, the pinch branch originating from $\mathbf{x}_D$ runs to the pure water vertex after changing its stability between saddle and node behavior several times, whereas the disjunct pinch branch connects the azeotrope and the ethanol pure component vertex. Hence, the reversible column can be used to obtain a high purity water product, but no ethanol may be produced. Obviously, the change of the specification $x_{D,water}$ has caused a shift in the connection of the singular points, i.e., the azeotrope and the pure component vertices by the pinch branches resulting in the accumulation of a different high-boiling component. The limiting condition of this shift is attained for some intermediate choice of the water content $x_{D,water} = z_{water}$ in the distillate product as shown in Figure 3c. The two pinch branches intersect at a ternary branching point. Both the ethanol and the water pure component vertices are accessible by a continuous reversible profile starting at $\mathbf{x}_D$. Hence, this distillate composition $\mathbf{x}_D = \mathbf{z}$ constitutes a point on the distillation boundary of a reversible column. Analogous to the definitions of the SDB and the CDB, this boundary is termed pinch distillation boundary (PDB), as it describes the limiting condition of the pinch map. The PDB for the ternary mixture acetone, ethanol, and water is shown with dotted lines in Figure 2.

Davydian et al.[41] investigate the boundary modes corresponding to this limiting condition of the pinch map and classify them with respect to the nonlinear analysis of equations systems as pitchfork bifurcations. They propose to calculate the point $\mathbf{z}$ on the boundary using a nonlinear set of equations of the form $\mathbf{f}(\mathbf{x}) = \mathbf{0}$, which includes the evaluation of a determinant. A summary of the application of bifurcation analysis for the determination of distillation regions can be found in Krolikowski.[42] Pöllmann and Blass[43] illustrate the graphical construction of $\mathbf{z}$ using the inflection

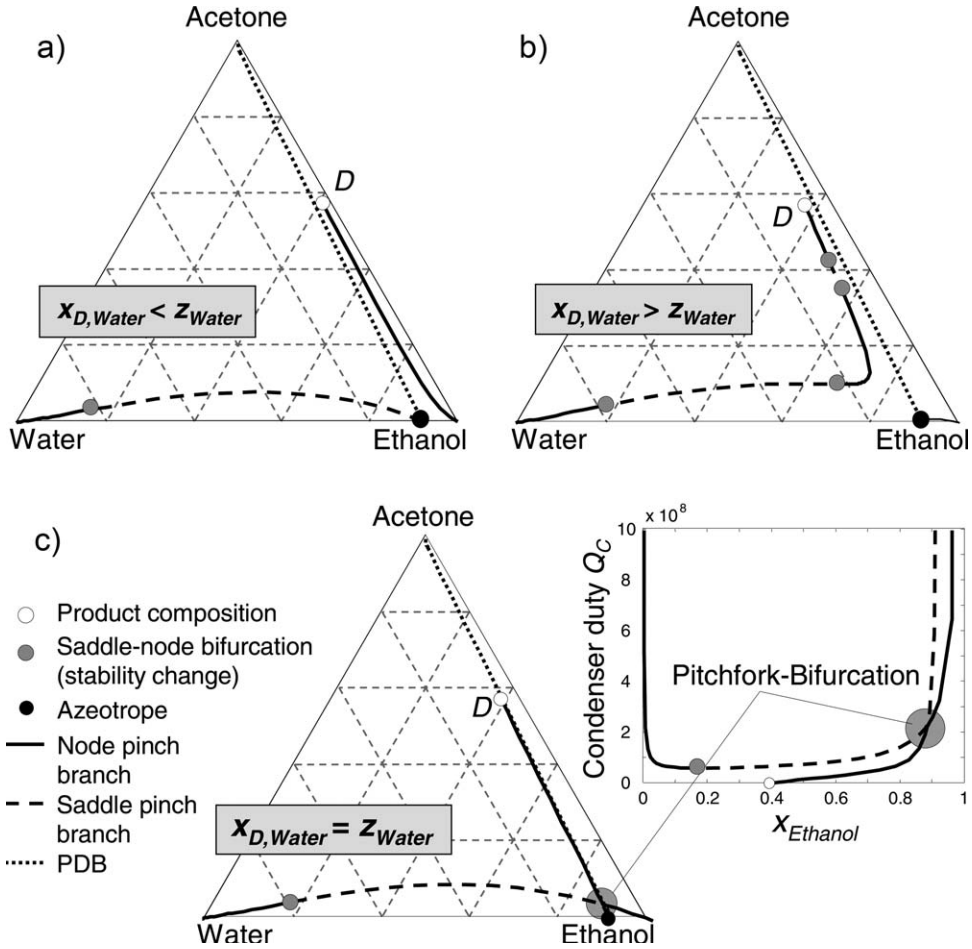


**Figure 3. Pinch maps of the rectifying section for three different specifications of the distillate composition $x_D$: (a) $x_{D,water} < z_{water}$, (b) $x_{D,water} > z_{water}$, and (c) $x_{D,water} = z_{water}$.**

The additional diagram in (c) shows the condenser heat duty (in W) along the pinch branches.

points of the pinch branches. In the context of the formulation of a feasibility test, the ability to locate point **z** on the boundary by solving a set of nonlinear equations is a very attractive property of the PDB. It is also a major distinction to SDB and CDB, where the determination of a point on the boundary is significantly more difficult and requires either a graphical inspection, a large number of trial-and-error calculations, or a precalculated data set of trajectories.

## Calculation of PDBs

The preceding discussion shows that the appearance of PDBs can be linked to a bifurcation phenomenon. In the following sections, an algorithm for the calculation of PDBs is developed. Their specific properties and the resulting consequences for the split feasibility assessment are discussed.

### *Bifurcation analysis*

We have argued above that any point **z** on the PDB is characterized by the appearance of a pitchfork bifurcation in the pinch map. Such link between the appearance of a pitchfork bifurcation and a significant switch in the behavior of a separation has also been observed for extractive distillation processes, where the appearance of a pitchfork bifurcation marks the minimum entrainer flow rate.[44] The calculation procedure used here for the determination of the PDB follows this earlier work.

First, the bifurcation point must comply with the set of pinch equations. For homogeneous, nonreactive mixtures the pinch equations are given by

$$0 = \bar{l}x_i + \bar{v}y_i - \alpha z_i, \quad i = 1, \ldots, C, \tag{2}$$

$$0 = y_i - K_i(\mathbf{x}, \mathbf{y}, T, p)x_i, \quad i = 1, \ldots, C, \tag{3}$$

$$0 = 1 - \sum_{k=1}^{C} x_k, \tag{4}$$

$$0 = 1 - \sum_{k=1}^{C} y_k, \tag{5}$$

$$0 = \alpha^2 + \bar{v}^2 - 1, \tag{6}$$

where $\bar{v} = \alpha v$, $\bar{l} = \alpha l$, and $l$, $v$ are the normalized liquid and vapor flow rates at the pinch point. The scaling factor $\alpha$ provides an ambiguous mapping $v \rightarrow (\alpha\bar{v})$ and $l \rightarrow (\alpha\bar{l})$, where

$l$, $v \in [-\infty,\infty]$ and $\bar{l}$, $\bar{v}$, $\alpha \in [-1,1]$. This specific form of modelling of $l$ and $v$ has favorable numerical properties if the pinch point lies close to one of the singular points of the residue curve map, i.e., the azeotropes and the pure component vertices, because the singular points are also pinch points at infinite reflux and, therefore, infinite liquid and vapor flows. For further information, we refer to Bausa.[45] For ease of reading, Eqs. 2–6 are abbreviated in the following sections by $\mathbf{f}_P(\mathbf{s}, \alpha, \mathbf{z})$, where $\mathbf{s} = (\mathbf{x}^T, \mathbf{y}^T, T, \bar{v}, \bar{l})^T$ holds all dependent variables, and $\alpha$, $\mathbf{z}$ are the remaining degrees of freedom of the pinch map.

A pitchfork bifurcation can be located on the manifold of pinch maps using a suitable test function.[46] The bifurcation point marks a change of stability on the pinch branches (cf. Figure 3c), which can be detected if the additional conditions

$$\mathbf{0} = \nabla_{\mathbf{s}} \mathbf{f}_P(\mathbf{s}, \alpha, \mathbf{z})^T \mathbf{w} \tag{7}$$

and

$$0 = \mathbf{w}^T \mathbf{w} - 1 \tag{8}$$

are appended to the set of Eqs. 2–6. Here, $\mathbf{w}$ is a null vector of $0 = \nabla_{\mathbf{s}} \mathbf{f}_P$. Furthermore, the pitchfork condition

$$0 = \nabla_{\alpha} \mathbf{f}_P(\mathbf{s}, \alpha, \mathbf{z})^T \mathbf{w} \tag{9}$$

must be fulfilled. Finally, the composition $\mathbf{z}$ on the boundary must obey the closure relation

$$0 = 1 - \sum_{k=1}^{C} z_k. \tag{10}$$

Eqs. 2–10 constitute $4C + 9$ equations with $5C + 7$ unknown variables. The locus of pitchfork bifurcations is thus parameterized by $C - 2$ degrees of freedom. In a ternary mixture, the manifold of the solutions forms a line. In the following, the system of equations given by Eqs. 2–10 is abbreviated by $\mathbf{F}_{\mathrm{PDB}}(\mathbf{z},\mathbf{t})$, where $\mathbf{t} = (\mathbf{x}^T, \mathbf{y}^T, T, \bar{v}, \bar{l}, \alpha, \mathbf{w}^T)^T$.

### *Evaluation of pitchfork branches*

To obtain a solution of the nonlinear set of equations, $\mathbf{F}_{\mathrm{PDB}}(\mathbf{z}, \mathbf{t}) = \mathbf{0}$ using a Newton-type local solver, suitable initial values for $\mathbf{z}$ and $\mathbf{t}$ must be known. In this context, it is useful to reconsider the special properties of the singular points ($\mathbf{x}_{\mathrm{sing}}$, $T_{\mathrm{sing}}$) of the residue curve map. Bausa[45] shows that these points correspond to pinch points at arbitrary reflux, i.e., they fulfil Eqs. 2–6 for $\mathbf{z} = \mathbf{x}_{\mathrm{sing}}$, $\mathbf{x} = \mathbf{x}_{\mathrm{sing}}$, $\mathbf{y} = \mathbf{x}_{\mathrm{sing}}$, and $T = T_{\mathrm{sing}}$. Further inspection of the local behavior of pinch branches close the singular points shows that they always change their stability at the singular point and that there are always at least two pinch branches intersecting at the singular point. Hence, there is a set of the flow parameters $\bar{v}$, $\bar{l}$, and $\alpha$ for which the additional conditions for the appearance of a pitchfork bifurcation in Eqs. 7–9 are fulfilled as well. The set of values can be obtained from a one-dimensional (1D) search in $\alpha$. Details are given in Appendix A. Frequently, an initialization with $\bar{l} = 1$, $\bar{v} = 1$, and $\alpha = 0$ is also sufficient. The null vector $\mathbf{w}$ corresponding to the directions of the pinch branches can be obtained from a singular value decomposition of the Jacobian of Eqs. 2–6. Hence, all singular points of the residue curve map represent valid solutions of $\mathbf{F}_{\mathrm{PDB}}(\mathbf{z}, \mathbf{t}) = \mathbf{0}$. This property is in fact not very surprising because the singular points are by definition also pitchfork bifurcations of the residue curves.

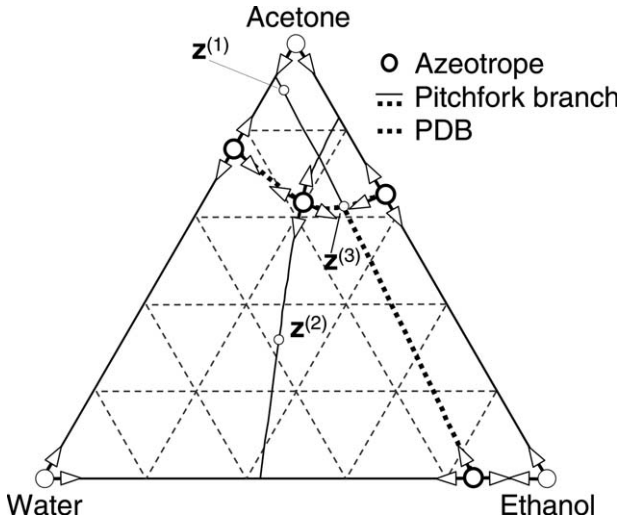


**Figure 4. Pitchfork branches at $p = 10$ atm.**

Using this insight, a complete pitchfork branch, i.e., a manifold of solutions $\mathbf{z}$, $\mathbf{t}$ with $\mathbf{F}_{\mathrm{PDB}}(\mathbf{z}, \mathbf{t}) = \mathbf{0}$, can be traced out using a suitable arc-length homotopy continuation algorithm. For the ternary example, mixture displaying one degree of freedom in $\mathbf{F}_{\mathrm{PDB}}(\mathbf{z}, \mathbf{t})$ and one element of the composition vector $\mathbf{z}$ is chosen as the continuation parameter. Figure 4 shows the complete set of the pitchfork branches at $p = 10$ atm. Note that both types of lines, e.g., the solid lines and the thick dotted lines, correspond to such branches. In total, 14 branches are found. They originate from the seven singular points in the directions of the respective null vectors, which are marked with arrows. Note that all binary edges of the composition space are pitchfork branches. Comparison of the pitchfork branches in Figure 4 with the PDBs in Figure 2 reveals that some of the pitchfork branches describe the PDB (thick dotted lines in Figure 4), whereas there are additional branches that cannot be linked to a PDB (solid lines in Figure 4). The branches on the binary edges may be interpreted as trivial distillation boundaries. For the branch originating at the ternary unstable node azeotrope (connecting the binary acetone–ethanol and ethanol–water edges) and for the upper part of the branch originating at the binary ethanol–water azeotrope above the intersection of the two PDBs, an interpretation is missing.

Figure 5 shows the pinch map for the compositions $\mathbf{z}^{(1)}$ and $\mathbf{z}^{(2)}$ on these two pitchfork branches. It can be seen that both pinch maps indeed give rise to a pitchfork bifurcation. Hence, they are valid solutions of $\mathbf{F}_{\mathrm{PDB}}(\mathbf{z}, \mathbf{t}) = \mathbf{0}$. In addition, the bifurcations are also located on a pinch branch that can be directly connected to the initial product compositions $\mathbf{z}^{(1)}$ and $\mathbf{z}^{(2)}$. However, in both cases, this product pinch branch passes through the ternary azeotrope before the pitchfork bifurcation is reached. On one hand, this azeotrope marks a pole of the pinch branch with respect to the reflux

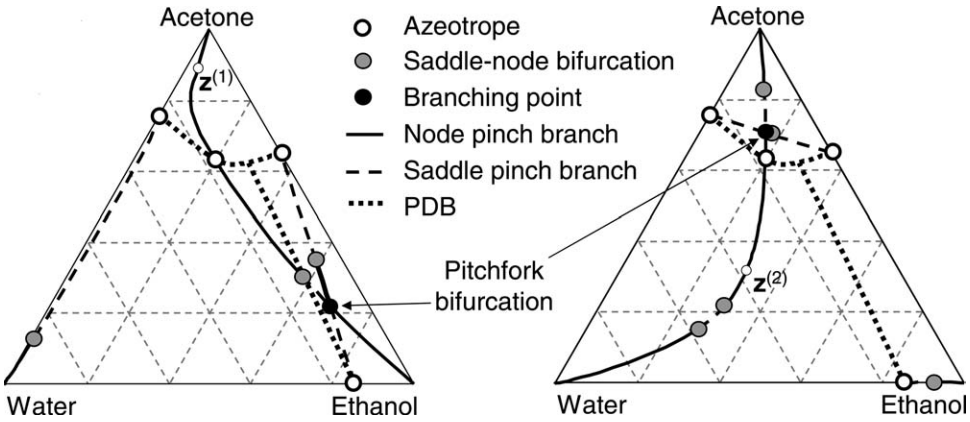


**Figure 5. Pinch maps for the product compositions $z^{(1)}$ (left) and $z^{(2)}$ (right) that are located on a pitchfork branch but not on a PDB.**

ratio. On the other hand, it also marks the boundary of the respective distillation region regardless whether SBD, CDB, or PDB are used. Hence, the pitchfork bifurcation marks a composition that can never be reached by the profile of a reversible column. Hence, the respective pitchfork branches do not carry any physical significance and can be omitted. In the following section, some rules for the determination of PDBs will be developed to avoid the calculation of physically insignificant pitchfork branches.

### *Rules for the determination of PDBs*

The pitchfork branches obtained from the homotopy continuation are governed by the choice of starting points. In the preceding section, all singular points and all of their null vectors have been used. This guarantees that all pitchfork branches with a connection to the singular points will be found. In principle, it is possible that isolated branches exist and are missed. However, even if such isolated branches exist they would probably not contribute to the PDBs. Instead, PDBs and SDB have been observed to always originate at saddle azeotropes. The pure component vertices only give rise to the trivial pitchfork branches on the edges of the composition space and thus can be omitted from the list of initial solutions. Node azeotropes like the ternary azeotrope in Figure 4 are passed by either one or more PDB and additional pitchfork branches without physical meaning. However, it is important to note that the PDB passing through the node azeotrope is already found from their origin at one of the saddle azeotropes. Hence, node azeotropes are also removed from the list of candidate starting points for PDB branches.

In addition to a limitation of the starting points to saddle azeotropes, only a subset of the null vectors need to be considered. For a binary minimum azeotrope like the ethanol–water azeotrope in Figure 4, only the stable eigenvector pointing in the direction of the ternary region and decreasing boiling temperatures needs to be considered. Correspondingly, only the unstable eigenvectors of maximum azeotropes pointing in the direction of increasing boiling temperatures are taken into account. Note that this strategy is not limited to ternary mixtures or binary azeotropes. The number and direction of unstable and stable eigenvectors of any azeotrope can be calculated by exploiting the eigeninformation of the equation system for detection of the azeotrope.

Reconsidering the continuation of the pitchfork bifurcations shown in Figure 4 using the guidelines for the selection of initial solutions discussed above, it is found that the amount of insignificant pitchfork paths that do not correspond to a PDB is greatly reduced. In fact, all continuation paths obtained by these rules contribute to a PDB. However, the section which holds $\mathbf{z}^{(1)}$ is still not removed correctly. Note that the corresponding pitchfork branch has a special property. It starts at the binary ethanol–water azeotrope and is a valid PDB until it intersects with the PDB connecting the other two binary azeotropes. The part above this point of intersection, however, does not correspond to a PDB. A straightforward strategy to avoid such behavior is to stop the continuation whenever an intersection with another PDB is detected. The corresponding set of equations is discussed in Appendix B.

Summarizing the discussion presented in Appendix B, it can be seen that the determination of the terminal point of a PDB is not only possible but also can be quite difficult. The formulation of a procedure for calculating this point based on homotopy continuation may be possible, but it is very likely that the procedure would lack robustness and be by far too complex to be used within an automated computational synthesis. It should be noted, however, that the additional part of the pitchfork branch starting from the azeotrope on the binary ethanol–water edge in Figure 4 does not influence the determination of the feasibility of a split in any of the two distillation regions containing this azeotrope. Correspondingly, the determination of the terminal point of the PDB using Eqs. B1–B9 is not required. This claim can be generalized under the assumption that a pitchfork branch will not re-enter the distillation region from which it originates after leaving it. Hence, a feasibility test based on the PDB can be formulated despite the difficulties in calculating the point of intersection of two boundaries.

### *Properties of PDBs*

The residue curves describing the SDB are known to follow a specific connectivity pattern. They always originate at a saddle azeotrope and end at some other singular point of

residue curve map. For the ternary mixture at $p = 10$ atm in Figure 2 (right), the three binary saddle azeotropes are all connected to the ternary node azeotrope. The PDBs, however, do not follow the same pattern. Although they originate at the saddle azeotropes as well they do not necessarily terminate at another azeotrope or a pure component vertex. In the example, only the two PDB originating at the binary acetone–ethanol and acetone–water azeotropes are connected to the ternary azeotrope. The PDB originating at the binary ethanol–water azeotrope terminates at a point roughly in the middle between the ternary and the binary acetone–ethanol azeotrope. As has already been discussed in the preceding section, this point marks an intersection of two PDB. A connection to the ternary azeotrope, which in principle should be reachable by distillation from any of the three distillation regions, can only be produced indirectly through the other PDB. Because of the different connectivity pattern of the PDB, some important implications on the distillation regions in the context of process design are observed.

The distillation regions confined by the PDB differ quantitatively from the ones that are formulated using the SDB. Often the difference is small, if not negligible, as for the distillation region containing the pure acetone vertex in Figure 2 (right). However, in other cases, a distillation region may be significantly enlarged, e.g., the one containing the water vertex or shrink, e.g., the one containing the ethanol vertex. Hence, the range of attainable distillate compositions for a split in the ethanol-rich distillation region is reduced if the PDB instead of the SDB are used for the evaluation of feasibility. For a distillate composition located between the PDB and the SDB (see bounded area in Figure 2, right), the assessments of the feasibility of the split given by PDB and SDB contradict. Distillate compositions in this area are feasible if the column is operated at infinite reflux and infeasible if the column is operated below the reflux ratio corresponding to the reversible separation. Between these two extreme modes of operation, the feasibility is a function of the reflux ratio. The impact of this region of ambiguous feasibility on finding the optimum operating point of a process is illustrated in detail in the second part of this series. However, it is important to note that the left part of the PDB between the binary acetone–ethanol azeotrope and the ternary azeotrope also belongs to the ethanol-rich distillation region in Figure 2 (right). Hence, all three distillation regions are accessible from any composition on this part of the PDB if a reversible column is used.

The connectivity pattern of the PDB can also result in different predictions of the feasibility of a split close to the binary edges of the composition space. At ambient pressure, the ternary mixture in Figure 2 (left) exhibits one distillation boundary originating from the binary ethanol–water azeotrope. The SDB connects this azeotrope to the acetone pure component vertex. Contrarily, the PDB terminates on the binary acetone–water edge (see cutout). Hence, it predicts that some compositions on this edge, which are heavy in acetone, can be produced in a column that operates in the ethanol-rich distillation region. Although the feasibility of such a split is only of theoretical interest for this mixture, it is a crucial property for the design of curved-boundary processes. A detailed example will be discussed in the second part of this series.

## Assessment of Split Feasibility

The determination of the PDBs builds the foundation for the development of a new algorithm for the assessment of the feasibility of the split in a simple distillation column. In the following sections, the conditions for split feasibility with respect to the PDB will be developed. These conditions will be used to formulate the feasibility algorithm, which needs the mass balance of the desired split as the only input, and does not require any visual check or manual intervention of the user and can be applied to mixtures with an arbitrary number of components. Hence, it is ideally suited for the integration into the optimization procedure for finding the best operating point, which is introduced in the second part of this series.

### *Observation of distillation boundaries*

The feasible operation of a simple distillation column requires that the given specifications for the distillate composition $\mathbf{x}_D$ and the composition of the bottom product $\mathbf{x}_B$ are connected by a continuous column profile. Hence, both product compositions must be located in the same distillation region.[10] Figure 6 (left) shows the mass balance line of a potential split, which will be used to illustrate the evaluation of the feasibility of a split.

In the example, the pure component vertices are arranged in the order of increasing boiling temperatures, i.e., component A is the light boiling component and component C is the heavy boiling component. The binary B–C mixture exhibits a minimum boiling azeotrope that gives rise to a ternary distillation boundary running from the azeotrope to the pure A vertex. The separation task in the column addresses the recovery of a high-purity C product $\mathbf{x}_{Fx}$ in the bottom of the column from a ternary feed. Hence, $\mathbf{x}_{Fx}$ marks a fixed product composition that should be attained in any case. Correspondingly, the split is confined to the left distillation region. At the top of the column, a binary A–B product $\mathbf{x}_{Fr}$ is desired, which is termed the free product composition. It can be seen that the mass balance line between the two products $\mathbf{x}_{Fx}$ and $\mathbf{x}_{Fr}$ intersects the distillation boundary. Hence, the desired split is infeasible.

Assuming for the moment that a split in the left distillation region (bounded by the pure A vertex, the azeotrope and the pure C vertex) is desired and the point of intersection $\mathbf{z}$ of the balance line and the distillation boundary is known, a geometrical feasibility criterion can be formulated.[47] The criterion is based on an evaluation of the distances $a$ between $\mathbf{z}$ and $\mathbf{x}_{Fx}$ and $b$ between $\mathbf{x}_{Fr}$ and $\mathbf{x}_{Fx}$, which are used as lever arms to form a feasibility indicator:

$$m = \frac{a}{b} = \frac{\|\mathbf{z} - \mathbf{x}_{Fx}\|}{\|\mathbf{x}_{Fr} - \mathbf{x}_{Fx}\|}, \tag{11}$$

The desired split is feasible with respect to the distillation boundary for $m \geq 1$, i.e., $\mathbf{x}_{Fr}$ is closer to $\mathbf{x}_{Fx}$ than to $\mathbf{z}$. Contrarily, the split in Figure 6 (left) with $m < 1$ is rated infeasible. It should be noted that the check for feasibility using the indicator $m$ presented here only refers to the observation of the distillation boundaries. However, this is only a necessary but not a sufficient criterion for the evaluation of

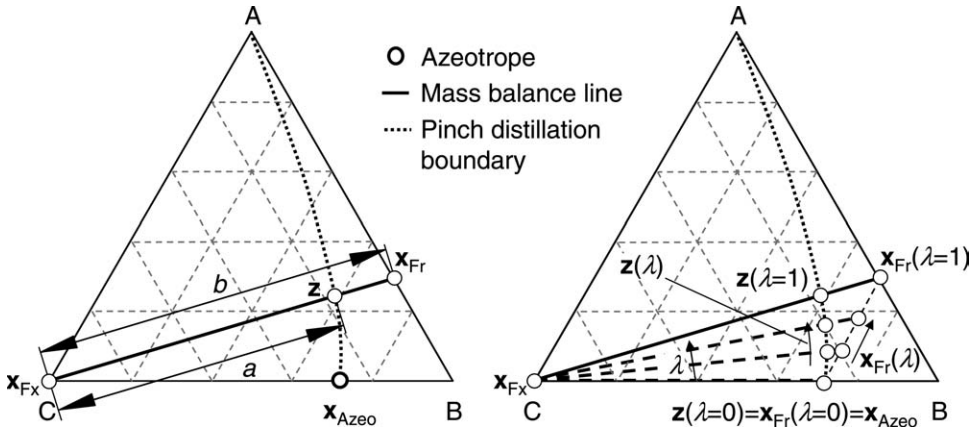


**Figure 6. Construction of the feasibility criterion *m* using the lever arm rule for an infeasible split (left) and determination of the corresponding composition z on the PDBs by homotopy continuation (right).**

feasibility of the specification of a column. Further requirements are presented in the following section.

To evaluate the feasibility indicator $m$, knowledge of the location of the point of intersection $\mathbf{z}$ of the mass balance line and the distillation boundary is vital. With respect to the definition of the lever arm rule, $\mathbf{z}$ must obey

$$0 = z_i - \big((1-m)x_{\mathrm{Fx},i} + m x_{\mathrm{Fr},i}\big), \quad i = 1, \ldots, C. \tag{12}$$

Using the PDB to describe the distillation boundaries, $\mathbf{z}$ can be obtained by solving a set of nonlinear equations given by the combination of Eq. 12 with Eqs. 2–9. Overall, the system of equations is characterized by $5C + 8$ unknowns ($\mathbf{t}$, $\mathbf{z}$, $m$) and the same number of equations. The set of equations can be solved reliably using a local solver if a good initialization is known.

Analogous to the calculation of a PDB, the saddle azeotropes of the mixture can be used to provide an initial solution. To use this initialization in the context of the feasibility test, the lever arm rule in Eq. 12 is replaced by a homotopy formulation

$$\begin{aligned} 0 = z_i &- \lambda\big((1-m)x_{\mathrm{Fx},i} + m x_{\mathrm{Fr},i}\big) \\ &-(1-\lambda)\big((1-m)x_{\mathrm{Fx},i} + m z_{0,i}\big), \quad i = 1, \ldots, C, \end{aligned} \tag{13}$$

where $\mathbf{z}_0 = \mathbf{x}_{\mathrm{Azeo}}$. At $\lambda = 0$ and $m = 1$, the balance line of the split is deformed to run from the fixed product $\mathbf{x}_{\mathrm{Fx}}$ to the azeotrope $\mathbf{x}_{\mathrm{Azeo}}$ with $\mathbf{x}_{\mathrm{Fr},\lambda=0} = \mathbf{x}_{\mathrm{Azeo}}$ (see Figure 6, right). A solution for Eqs. 2–9 is given by $\mathbf{t}_0 = (\mathbf{x} = \mathbf{y} = \mathbf{z} = \mathbf{x}_{\mathrm{Azeo}}, T = T_{\mathrm{Azeo}}, \bar{l}_0, \bar{v}_0, \alpha_0, \mathbf{w} = \mathbf{w}_0)$, where $\bar{l}_0$, $\bar{v}_0$, and $\alpha_0$ are obtained as described in Appendix A, and $\mathbf{w}_0$ is the corresponding null vector. The balance line can then be moved iteratively to the desired free product $\mathbf{x}_{\mathrm{Fr}}$ at $\lambda = 1$. Figure 6 (right) shows the path of the continuation in the ternary diagram. In this specific case, it is sufficient to perform the calculation using the unstable eigenvector of the azeotrope because the distillation boundary associated to the stable eigenvector is identical to the binary B–C edge. For a ternary azeotrope, however, two separate continuation runs for both eigenvectors are necessary. For mixtures with more than one nontrivial distillation boundary, each saddle azeotrope $\mathbf{x}^j_{\mathrm{azeo}}$ is the starting point for a continuation run resulting in a feasibility indicator $m^j$. Overall feasibility of the split with respect to the observation of the distillation boundaries is then subject to the smallest positive value $m^j$.

### *Definition of fixed and free product compositions*

Considering the formulation of the lever arms in Eq. 11, the classification of the two desired product compositions into a fixed product composition $\mathbf{x}_{\mathrm{Fx}}$ and a free product composition $\mathbf{x}_{\mathrm{Fr}}$ has a large impact on the feasibility indicator $m$. The classification defines

(1) the distillation region of the separation, i.e., the distillation region containing $\mathbf{x}_{\mathrm{Fx}}$,

(2) which lever arm between $\mathbf{z}$ and a product composition is used to determine $m$, i.e., the one between $\mathbf{z}$ and $\mathbf{x}_{\mathrm{Fx}}$.

The decision on $\mathbf{x}_{\mathrm{Fx}}$ and $\mathbf{x}_{\mathrm{Fr}}$ is governed by the desired separation task. In this example, the task is the recovery of high-purity C in the fixed product $\mathbf{x}_{\mathrm{Fx}}$, whereas the free product $\mathbf{x}_{\mathrm{Fr}}$ may be changed to accommodate feasibility with respect to the distillation boundary or any other constraint formulated in the synthesis problem. In the context of synthesis, the definition of fixed and free products by formulation of separation tasks is easily obtained for all columns, which produce an external product of the process. For a pressure-swing process for the separation of ethanol and water using acetone as a light-boiling entrainer (cf. distillation boundaries in Figure 2), the bottom products of both columns are fixed products, i.e., high-purity water in C1 and high-purity ethanol in C2.

As stated above, the observation of the distillation boundaries is a necessary but not a sufficient criterion for split feasibility. In addition, the desired products $\mathbf{x}_{\mathrm{Fx}}$ and $\mathbf{x}_{\mathrm{Fr}}$ can only be achieved if they correspond to a thermodynamically sensible distribution of the feed composition into a light product, $\mathbf{x}_{\mathrm{Fr}}$, and a heavy product, $\mathbf{x}_{\mathrm{Fx}}$. For zeotropic mixtures, the concept of light and heavy keys is frequently applied[48] to determine this distribution. It states that all components that have a lower boiling point than the light key must accumulate completely in the distillate product, whereas all components that have a higher boiling point than

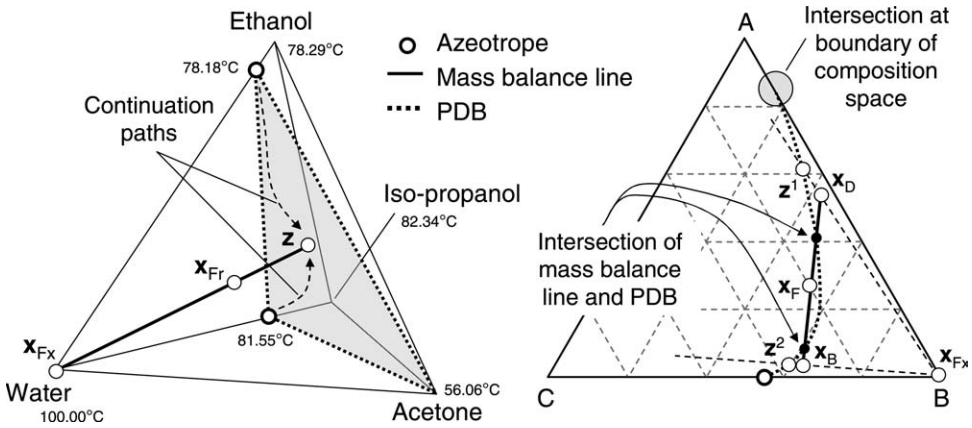


**Figure 7. Continuation paths for the determination of z for a quaternary mixture (left) and illustration of limitations of the feasibility check (right).**

the heavy key must accumulate completely in the bottom product. Light and heavy keys are components with adjacent boiling points. Hence, the separation task can be regarded as pseudobinary by lumping all heavy nonkey components to the heavy key and all light nonkey components to the light key. The concept of key components can also be transferred to azeotropic systems if the azeotropes are treated as pseudocomponents. In the following, all separation tasks will be formulated such that a consistent distribution of the lights and heavies is observed.

### *Feasibility algorithm*

Based on the theory of the assessment of the feasibility criteria and the procedure for calculating the feasibility indicator $m$, a general-purpose algorithm for the assessment of the feasibility of a desired azeotropic split is developed. It can be summarized as follows:

*Procedure 1*

(1) Specify the fixed product composition $\mathbf{x}_{Fx}$ according to the separation task.
(2) Specify the free product composition $\mathbf{x}_{Fr}$.
(3) Confirm whether $\mathbf{x}_{Fx}$ and $\mathbf{x}_{Fr}$ comply with the concept of key components. Azeotropes are treated as pseudocomponents. Otherwise, the split is considered infeasible.
(4) Assemble a list of all saddle azeotropes $\mathbf{x}_{SA}^{j}$, $j = 1, \ldots, N_{SA}$, in the distillation region of the fixed product composition $\mathbf{x}_{Fx}$ to be used as starting points for the PDB branches.
(5) Determine the point of intersection $\mathbf{z}$ of the mass balance line defined by $\mathbf{x}_{Fx}$ and $\mathbf{x}_{Fr}$ with the boundaries of the composition space. Calculate $m^1 = m$ from Eq. 11 using this composition $\mathbf{z}$. Set $K = 1$.
(6) For $j = 1, \ldots, N_{SA}$ do:
   (a) Determine $\mathbf{z}^j$ from homotopy continuation starting from $\mathbf{x}_{SA}^{j}$ in the direction of a linear combination of the unstable eigenvectors and in the direction of a linear combination of the stable eigenvectors of the azeotrope. If the azeotrope does not have a nontrivial unstable or stable eigenvector, i.e., an eigenvector that does not fall together with boundary of the composition space, the continuation in the respective direction can be omitted. If no intersection $\mathbf{z}^j$ is found, skip Step 6(b) and continue with the next azeotrope.
   (b) Calculate $m$ from Eq. 11 using $\mathbf{z}^j$ from the homotopy continuation. If $m > 0$ increase $K$ by one and set $m^K = m$.
(7) Set $m = \min(m^k)$, where $k = 1, \ldots, K$ to consider the closest boundary for the feasibility indicator $m$.

The feasibility algorithm has been implemented in a conceptual design software package. Details on the implementation and illustrative examples for the application of the feasibility algorithm can be found elsewhere.[49] However, some elements of the algorithm presented above are still missing in the current implementation. Currently, the compliance of the product compositions $\mathbf{x}_{Fx}$ and $\mathbf{x}_{Fr}$ with the concepts of key components in Step 3 is not checked. Hence, it is the responsibility of the user to supply consistent specifications to the feasibility test. As the overwhelming majority of separation tasks demands the purification of a pure component, an azeotropic composition or a mixture thereof the rule is easily fulfilled.

A crucial step of the algorithm is the selection of the starting points for the homotopy continuation in Step 4. On one hand, the list must be compiled such that at least one saddle azeotrope on each separate distillation boundary is supplied. On the other hand, continuation runs originating from saddle azeotropes in different distillation regions may lead to an erroneous assessment of feasibility due to the determination of compositions $\mathbf{z}$, which lie on a physically meaningless pitchfork continuation path. Hence, they should not appear in the list of starting points. Currently, the list of starting points is supplied by the user. However, it should be noted that it can also be created automatically from an analysis of the topology of the mixture. As a matter of fact, all saddle azeotropes in the respective distillation region can be taken from the reachability matrix introduced by Rooks et al.[17] The information contained in this matrix can also be used to limit the list to the minimum number of saddle azeotropes, which are

necessary to access all distillation boundaries. For example, Figure 7 (left) shows the nearly planar distillation boundary surface of the quaternary mixture of acetone, ethanol, isopropanol, and water at $p = 1$ atm.

The surface originates at the two binary saddle azeotropes on the binary alcohol–water edges. Both azeotropes are valid starting points for the homotopy computation of a composition $\mathbf{z}^j$ on the boundary, which is necessary to assess the feasibility indicator $m$ of the split given by $\mathbf{x}_{Fx}$ and $\mathbf{x}_{Fr}$. Potential continuation paths are sketched in the figure. However, as both azeotropes lie on the same boundary, both continuation runs would end at the same composition $\mathbf{z}$. Hence, it is sufficient to have one of the azeotropes on the list of the potential starting points.

### *Limitations of the feasibility test*

The feasibility algorithm implicitly assumes that there is at most one point of intersection $\mathbf{z}$ between the mass balance line of the separation and one single PDB. This assumption is fulfilled whenever the feed composition $\mathbf{x}_F$ is located in the same distillation region as the distillate and bottom product compositions $\mathbf{x}_D$ and $\mathbf{x}_B$. This is the case for the overwhelming majority of splits in industrially relevant processes. However, processes based on the exploitation of a highly curved distillation boundary present an important exception (cf. Figure 1). Their successful application depends on at least one split in which $\mathbf{x}_F$ is located in a different region from $\mathbf{x}_D$ and $\mathbf{x}_B$. Wahnschafft et al.[31] use the term ''boundary crossing'' for this class of splits.

Figure 7 (right) shows the mass balance line of a feasible split specification that involves boundary crossing. Note that two points of intersection with the PDB are found on the mass balance line between $\mathbf{x}_D$ and $\mathbf{x}_B$. Application of Eq. 11 in Step 6(b) of the feasibility algorithm with any one of these points of intersection will result in a feasibility indicator $m < 1$. Hence, the split is erroneously rated as infeasible.

At this point, it should be stressed that a reformulation of the algorithm, which accommodates splits with boundary crossing, appears manageable and can be expected to involve merely a small amount of additional computation. However, the development of such reformulation shall be left to future research. At this point, a more pragmatic strategy for the treatment of boundary crossing is applied. To illustrate this strategy in Figure 7 (right), imagine pure B is to be recovered from $\mathbf{x}_F$. First, the fixed composition $\mathbf{x}_{Fx}$ is set to the target composition of the boundary crossing operation and its potential downstream columns. Therefore, in case of the example, $\mathbf{x}_{Fx}$ is located at the pure B vertex. Second, two feasibility checks according to the feasibility algorithm are introduced with $\mathbf{x}_{Fr} = \mathbf{x}_D$ and $\mathbf{x}_{Fr} = \mathbf{x}_B$, respectively. For the example in Figure 7 (right), the points $\mathbf{z}^{(1)}$ and $\mathbf{z}^{(2)}$ on the PDB and, correspondingly, a correct assessment of the feasibility are obtained.

## Conclusions

A geometric feasibility check for azeotropic separations based on bifurcation theory has been developed. A closed-form representation of the distillation boundaries is obtained by continuation of pitchfork bifurcation points of the pinch map. The feasibility check is general and can be applied to arbitrary azeotropic mixtures. As it does not require visualization or manual graphical checks, it can be used without limitations regarding the number of components or certain types of splits.

The algorithm of the feasibility check is fully computational. In addition to giving a yes-or-no assessment of the feasibility of a proposed split, it also calculates the distance of the specified column products from the boundaries. Hence, it provides additional sensitivity information regarding the placement of the product compositions. Because of these properties, the new feasibility check is ideally suited for use within an optimization framework for the fast economic assessment and the determination of the optimal operating point of a given separation configuration. The second part of this series will focus on the formulation of such an optimization framework. Several ternary and quaternary examples will highlight the versatility of the feasibility check within the optimization framework.

Even though the feasibility test presented here has been developed as part of a general optimization framework for separation processes, it is important to note that it can also be used as a valuable stand-alone tool, for example, during the phase of the qualitative design of alternative flow sheets for a given separation task. It enables to quickly explore different options of potential splits computationally. It is especially helpful if the mixture at hand is multicomponent and multiazeotropic and, hence, cannot be reduced to a ternary mixture by lumping of components without loss of critical information about the topology.

Within the scope of this article, the formulation of the feasibility check has been limited to homogeneous mixtures. However, first investigations of the heterogeneous mixture acetone–water–toluene suggest that the underlying bifurcation-theoretic observations can likely be transferred to heterogeneous and reactive mixtures as well.[49] Future work will deal with the extension of the feasibility check to these kinds of mixtures.

## Literature Cited


1. DeVilliers WE, French RN, Koplos GJ. Navigate phase equilibria via residue curve maps. *Chem Eng Prog*. 2002;98:66–71.
2. Matsuyama H, Nishimura H. Topological and thermodynamic classification of ternary vapor-liquid equilibria. *J Chem Eng Jpn*. 1977; 10:181–187.
3. Doherty MF, Calderola GA. Design and synthesis of homogeneous azeotropic distillations: 3. The sequencing of columns for azeotropic and extractive distillations. *Ind Eng Chem Fundam*. 1985;24:474–485.
4. Barburina LV, Platonov VM, Slinko MG. Classification of vapor-liquid phase diagrams for homoazeotropic systems. *Theo Found Chem Eng*. 1988;22:390–396.
5. Hilmen EK, Skogestad S. Topology of ternary VLE diagrams: elementary cells. *AIChE J*. 2002;48:752–759.
6. Kiva VN, Hilmen EK, Skogestad S. Azeotropic phase equilibrium diagrams: a survey. *Chem Eng Sci*. 2003;58:1903–1953.
7. Stichlmair JG, Fair JR. *Distillation: Principles and Practices*. New York: Wiley, 1998.
8. Manan ZA, Banares-Alcantara R. A new catalog of the most promising separation sequences for homogeneous azeotropic mixtures: I. Systems without boundary crossing. *Ind Eng Chem Res*. 2001;40: 5795–5809.

9. Stichlmair JG, Herguijuela JR. Separation regions and processes of zeotropic and azeotropic ternary distillation. *AIChE J*. 1992;38: 1523–1535.
10. Doherty MF, Malone MF. *Conceptual Design of Distillation Systems*. New York: McGraw-Hill, 2001.
11. Pham HN, Doherty MF. Design and synthesis of heterogeneous azeotropic distillations: I. Heterogeneous phase diagrams. *Chem Eng Sci*. 1990;45:1823–1836.
12. Pham, HN, Doherty MF. Design and synthesis of heterogeneous azeotropic distillations: II. Residue curve maps. *Chem Eng Sci*. 1990; 45:1837–1843.
13. Barbosa D, Doherty MF. The simple distillation of homogeneous reactive mixtures. *Chem Eng Sci*. 1988;43:541–550.
14. O'Young LY, Natori T, Pressly G, Ng KM. A physical limitation based framework for separation synthesis. *Comp Chem Eng*. 1997;21:S223–S230.
15. Levy SG, van Dongen DB, Doherty MF. Design and synthesis of homogeneous azeotropic distillations: 2. Minimum reflux calculations for nonideal and azeotropic columns. *Ind Eng Chem Fundam*. 1985;24:463–474.
16. Jaksland CA, Gani R, Lien KM. Separation process design and synthesis based on thermodynamic insights. *Chem Eng Sci*. 1995;50: 511–530.
17. Rooks RE, Julka V, Doherty MF, Malone MF. Structure of distillation regions for multicomponent azeotropic mixtures. *AIChE J*. 1998;44:1382–1391.
18. Ryll O, Blagov S, Hasse F. Rechnergestützter konzeptioneller Entwurf von Destillations-/Reaktionsprozessen. *Chem Ing Tech*. 2008;80:207–213.
19. Wibowo C, Ng KM. Visualization of high-dimensional phase diagrams of molecular and ionic mixtures. *AIChE J*. 2002;48:991–1000.
20. Harjo B, Ng KM, Wibowo C. Visualization of high-dimensional liquid–liquid-equilibrium phase diagrams. *Ind Eng Chem Res*. 2004;43: 3566–3576.
21. Lucia A, Taylor R. The geometry of separation boundaries: I. Basic theory and numerical support. *AIChE J*. 2006;52:582–594.
22. Taylor R, Miller A, Lucia A. The geometry of separation boundaries: systems with reaction. *Ind Eng Chem Res*. 2006;45:2777–2786.
23. Bellows M, Lucia A. The geometry of separation boundaries: four component mixtures. *AIChE J*. 2007;53:1770–1778.
24. Lucia A, Taylor R. The geometry of separation boundaries: II. Mathematical formalism. *AIChE J*. 2006;53:1779–1788.
25. Lucia A, Amale A, Taylor R. Energy efficient hybrid separation processes. *Ind Eng Chem Res*. 2006;45:8319–8328.
26. Lucia A, Amale A, Taylor R. Distillation pinch points and more. *Comp Chem Eng*. 2008;32:1342–1364.
27. Zhang LB, Linninger AA. Towards computer-aided separation synthesis. *AIChE J*. 2006;52:582–594.
28. Vogelpohl, A. Definition von Destillationslinien bei der Trennung von Mehrstoffgemischen. *Chem Ing Tech*. 1993;65:515–522.
29. Safrit BT, Westerberg AW. Algorithm for generating the distillation regions for azeotropic multicomponent mixtures. *Ind Eng Chem Res*. 1997;36:1827–1840.
30. Pöpken T, Gmehling J. Simple method for determining the location of distillation region boundaries in quaternary systems. *Ind Eng Chem Res*. 2004;43:777–783.
31. Wahnschafft OM, Koehler JW, Blass E, Westerberg AW. The product composition regions of single-feed azeotropic distillation columns. *Ind Eng Chem Res*. 1992;31:2345–2362.
32. Liu G. Synthesis of Multicompnent Azeotropic Distillation Sequences. Ph.D. thesis, University of Manchester of Science and Technology (UMIST), Manchester, 2004.
33. Blagov S, Hasse H. Topological analysis of vapor–liquid equilibrium diagrams for distillation process design. *Phys Chem Chem Phys*. 2002;4:896–908.
34. Alba-Argaez. *Distil 5.0 Reference Manual*. Aspentech/Hyprotech, 1999.
35. Vogelpohl A. Rektifikation von Dreistoffgemischen. Teil 2: Rektifikationslinien realer Gemische und Berechnung der Dreistoffrektifikation. *Chem Ing Tech*. 1964;36:1033–1045.
36. Nikolaev NS, Kiva VN, Mozzhukin AS, Serafimov LA, Goloborodkin SI. Utilization of functional operators for determining the regions of continuous rectification. *Theo Found Chem Eng*. 1979; 13:418–431.
37. Fidkowski ZT, Doherty MF, Malone MF. Feasibility of separations for distillation of nonideal ternary mixtures. *AIChE J*. 1993;39: 1303–1321.
38. Bausa J, von Watzdorf R, Marquardt W. Shortcut methods for nonideal multicomponent distillation: 1. Simple columns. *AIChE J*. 1998;44:2181–2198.
39. Urdaneta RY, Bausa J, Brüggemann S, Marquardt W. Analysis and conceptual design of ternary heterogeneous azeotropic distillation processes. *Ind Eng Chem Res*. 2002;41:3849–3866.
40. Köhler J, Aguirre P, Blass E. Minimum reflux calculations for nonideal mixtures using the reversible distillation model. *Chem Eng Sci*. 1991;49:3325–3330.
41. Davydian AG, Malone MF, Doherty MF. Boundary modes in a single feed distillation column for the separation of azeotropic mixtures. *Theo Found Chem Eng*. 1997;31:327–338.
42. Krolikowski LJ. Determination of distillation regions for non-ideal ternary mixtures. *AIChE J*. 2006;52:532–544.
43. Pöllmann P, Blass E. Best products of homogeneous azeotropic distillations. *Gas Sep Purif*. 1994;8:194–228.
44. Brüggemann S, Marquardt W. Shortcut methods for nonideal multicomponent distillation: 3. Extractive distillation columns. *AIChE J*. 2004;50:1129–1149.
45. Bausa J. Näherungsverfahren für den konzeptionellen Entwurf und die thermodynamische Analyse von destillativen Trennprozessen. Ph.D. thesis, Lehrstuhl für Prozesstechnik, RWTH Aachen in. In: Fortschrittberichte VDI, Reihe 3, Nr. 692. Düsseldorf: VDI Verlag, 2001.
46. Beyn WJ, Champneys A, Doedel E, Govaerts W, Kuznetsov YA, Sanstede B. *Numerical continuation and computation of normal forms*. In: Fiedler B, editor. *Handbook of Dynamical Systems*, vol.2. Amsterdam: Elsevier, 2002:149–219.
47. Brüggemann S, Marquardt W. *Design and optimization of recycle policies for multicomponent azeotropic distillation processes with bifurcation analysis*. In: Barbarosa-Povoa A, Matos H, editors. *European Symposium on Computer Aided Process Engineering–14*. Amsterdam: Elsevier, 2004:349–354.
48. King CJ. *Separation Processes*. New York: McGraw-Hill, 1980.
49. Brüggemann S. Rapid Screening of Conceptual Design Alternatives for Distillation Processes. Ph.D. thesis, Lehrstuhl für Prozesstechnik, RWTH Aachen in. In: Fortschrittberichte VDI, Reihe 3, Nr. 841. Düsseldorf: VDI Verlag, 2005.

## Appendix A: 1D Search in $\alpha$ for Initializing the PDB Homotopy

The calculation of the pitchfork branches using homotopy continuation requires that suitable initial solutions $\mathbf{t}_0 = (\mathbf{x}_0, \mathbf{y}_0, T_0, \bar{v}_0, \bar{l}_0, \alpha_0, \mathbf{w}_0)$ of the pitchfork bifurcation equation system $\mathbf{F}_{\mathrm{PDB}}(\mathbf{z}, \mathbf{t})$ in Eqs. 2–10 are known. According to the discussion on the evaluation of pinch branches, such initial solutions $\mathbf{t}_0$ exist at all singular points of the residue curve map. However, in the context of the determination of the PDB, it is sufficient to consider only the initial solutions $\mathbf{t}_0$ at the saddle azeotropes. The positioning of $\mathbf{t}_0$ at a singular point of the residue curve map corresponds to $\mathbf{z}_0 = \mathbf{x}_{\mathrm{sing}}$, $\mathbf{x}_0 = \mathbf{x}_{\mathrm{sing}}$, $\mathbf{y}_0 = \mathbf{x}_{\mathrm{sing}}$, and $T_0 = T^B(\mathbf{x}_{\mathrm{sing}}, p)$. Note that for this choice of $\mathbf{z}_0$, $\mathbf{x}_0$, and $\mathbf{y}_0$ the mass balance of Eq. 2 becomes singular. Hence, the set of pinch Eqs. 2–6 is fulfilled trivially for all sets of $\alpha_0$ and $\bar{v}_0$, which obey Eq. 6, and a corresponding choice of $\bar{l}_0$. The composition of the singular point automatically marks a pinch point regardless of the reflux ratio $r$, which can be directly calculated from $\alpha$, $\bar{v}$, and $\bar{l}_0$. Correspondingly, there must exist a singular pinch branch at this composition.

It is important to note that adherence to the set of pinch Eqs. 2–6 is only a necessary but not a sufficient criterion for solving the pitchfork bifurcation system given by Eqs. 2–10.

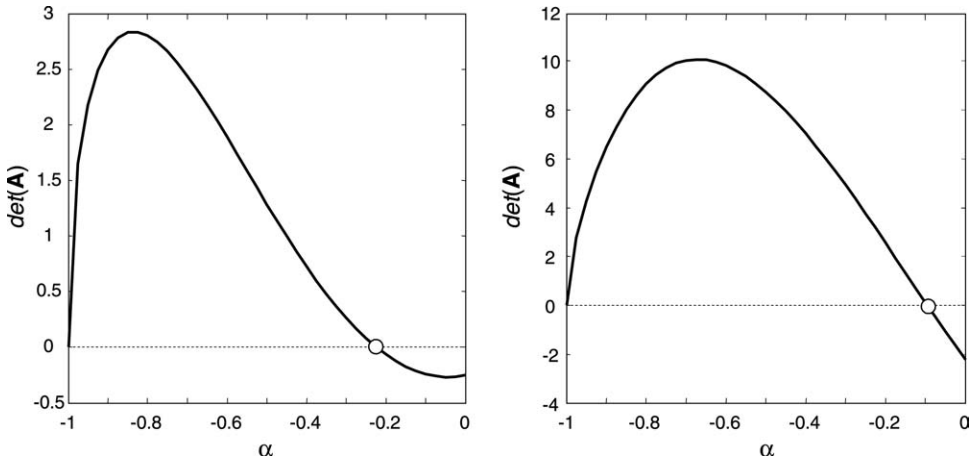


**Figure A1. Determinant det(A) as a 1D function of $\alpha$ at $p = 1$ atm for the binary isopropanol–water (left) and the binary ethanol–water (right) azeotropes.**

In addition, Eqs. 7 and 8 require that the matrix $\mathbf{A} = \bigtriangledown_{\mathbf{s}}\mathbf{f}_P(\mathbf{s},\alpha,\mathbf{z})$ is singular, i.e., $\det(\mathbf{A}) = 0$. An analysis of the derivatives of Eq. 2 with respect to $\mathbf{x}$ and $\mathbf{y}$ indicates that this additional criterion is not independent of $\alpha$, $\bar{v}$, and $\bar{l}$. It can be concluded that a robust continuation of pitchfork branches is only guaranteed if $\alpha$, $\bar{v}$, and $\bar{l}$ are chosen such that the additional criterion $\det(\mathbf{A}) = 0$ is fulfilled. Note that $\bar{v}$ can be interpreted as a function of $\alpha$ using Eq. 6. However, $\bar{v}(\alpha)$ is only unique with respect to the absolute value of $\bar{v}$ but not with respect to the sign. The sign indicates whether the set of pinch point equations are solved for the rectifying section ($\alpha$ and $\bar{v}$ are negative) or the stripping section ($\alpha$ and $\bar{v}$ are positive; cf. Bausa[45]). In other words, a negative sign corresponds to the calculation of pinch branches in the direction of increasing temperatures from the product composition $\mathbf{z}$, whereas a positive sign indicates a calculation in the direction of decreasing temperatures. For the calculation of the pitchfork branches, the signs of $\alpha$ and $\bar{v}$, correspondingly, indicate whether the PDB is continued toward increasing (negative sign) or decreasing temperatures (positive sign). For a given direction of the continuation, $\bar{v}(\alpha)$ with

$$\bar{v} = \text{sign}(\text{direction})\sqrt{1-\alpha^2}, \tag{A1}$$

is unique. Furthermore,

$$\bar{l} = -\text{sign}(\text{direction})\left(\alpha + \sqrt{1-\alpha^2}\right), \tag{A2}$$

expresses $\bar{l}$ as a function of $\alpha$ using the summation of Eq. 2 for all components $i = 1, \ldots, C$ in combination with the definition in Eq. A1.

Using the definitions in Eqs. A1 and A2, the additional criterion for the initial solution of the pitchfork continuation $\det(\mathbf{A}) = 0$ is a 1D function of $\alpha$. Figure A1 shows the graph of $\det(\mathbf{A}(\alpha))$ at $p = 1$ atm for the binary isopropanol–water (left) and the binary ethanol–water (right) azeotropes.

Both azeotropes are minimum boiling. Hence, the PDB is found by continuation toward increasing temperatures such that $-1 \leq \alpha \leq 0$. In case of the isopropanol–water azeotrope (Figure A1, left), it can be seen that additional criterion $\det(\mathbf{A}) = 0$ is fulfilled at $\alpha = -0.225$. Moreover, it is also fulfilled trivially at $\alpha = -1$. However, this trivial root is physically insignificant because it describes a column with a vanishing vapor flow rate $\bar{v} = 0$, i.e., essentially a tube. Hence, $\alpha_0 = -0.225$ marks the initial solution $(\mathbf{z}_0, \mathbf{t}_0) = (\mathbf{z}_0 = \mathbf{x}_{\text{sing}}, \mathbf{x}_0 = \mathbf{x}_{\text{sing}}, \mathbf{y}_0 = \mathbf{x}_{\text{sing}}, T_0 = T_{\text{sing}}, \bar{v}_0 = \bar{v}(\alpha_0), \bar{l}_0 = \bar{l}(\alpha_0), \alpha_0, \mathbf{w}_0 = \mathbf{w}(\mathbf{A}))$ of the pitchfork continuation. The null vector $\mathbf{w}_0$ is obtained from a singular value decomposition of the Jacobian $\mathbf{A}$. For the ethanol–water azeotrope (Figure A1, right), a nontrivial root of $\det(\mathbf{A})$ is found at $\alpha_0 = -0.095$. Hence, the initial solution of the pitchfork bifurcation is given by $(\mathbf{z}_0, \mathbf{t}_0) = (\mathbf{z}_0 = \mathbf{x}_{\text{sing}}, \mathbf{x}_0 = \mathbf{x}_{\text{sing}}, \mathbf{y}_0 = \mathbf{x}_{\text{sing}}, T_0 = T_{\text{sing}}, \bar{v}_0 = \bar{v}(\alpha_0), \bar{l}_0 = \bar{l}(\alpha_0), \alpha_0, \mathbf{w}_0 = \mathbf{w}(\mathbf{A}))$.

In summary, it can be concluded that the values of $\alpha$, $\bar{v}$, and $\bar{l}$ at an initial solution $(\mathbf{z}_0, \mathbf{t}_0)$ corresponding to a singular point $\mathbf{z}_0 = \mathbf{x}_{\text{sing}}$ of the residue curve map, e.g., at a saddle azeotrope, can be found by a 1D search in $\alpha$. However, it should be noted that the additional criterion $\det(\mathbf{A}) = 0$ is, in principle, still not sufficient. As a final criterion, the pitchfork condition in Eq. 9 must also be fulfilled. However, this final criterion is fulfilled trivially for the two examples shown above. Nevertheless, it may be of importance if multiple candidates of initial solutions are found by the 1D search for roots of $\det(\mathbf{A})$. In such case, the final criterion can be used to discriminate the real initial solution from these candidates. However, such situation, if possible at all, seems to be rare as it has not yet been encountered.

## Appendix B: Locating an Intersection Point of Two PDB

Figure B1 shows the pinch map at the point of intersection $\mathbf{z}^{(3)}$ of the two PDB (cf. Figure 4). It can be seen that two pitchfork bifurcations located at $(\mathbf{s}_1, \alpha_1, \mathbf{w}_1)$ and $(\mathbf{s}_2, \alpha_2, \mathbf{w}_2)$, respectively, can be found. They are connected to the product composition $\mathbf{z}^{(3)}$ of the pinch equations. Both of these pitchfork bifurcations can be detected separately using Eqs. 2–9. In addition, the closure relation in Eq. 10 must be fulfilled as well. Hence, the point of intersection $\mathbf{z} = \mathbf{z}^{(3)}$ must comply with

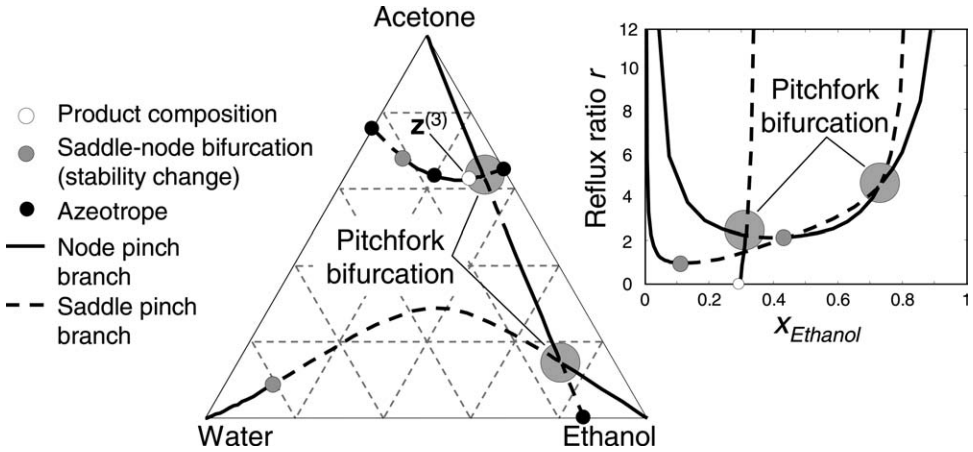


**Figure B1. Pinch map for the product composition $\mathbf{z}^{(3)}$, which is characterized by the intersection of two pitchfork branches.**

$$\mathbf{0} = \mathbf{f}_P(\mathbf{s}_1, \alpha_1, \mathbf{z}), \tag{B1}$$

$$\mathbf{0} = \nabla_{\mathbf{s}_1}\mathbf{f}_P(\mathbf{s}_1, \alpha_1, \mathbf{z})^T\mathbf{w}_1, \tag{B2}$$

$$0 = \mathbf{w}_1^T\mathbf{w}_1 - 1, \tag{B3}$$

$$0 = \nabla_{\alpha_1}\mathbf{f}_P(\mathbf{s}_1, \alpha_1, \mathbf{z})^T\mathbf{w}_1, \tag{B4}$$

$$\mathbf{0} = \mathbf{f}_P(\mathbf{s}_2, \alpha_2, \mathbf{z}), \tag{B5}$$

$$\mathbf{0} = \nabla_{\mathbf{s}_2}\mathbf{f}_P(\mathbf{s}_2, \alpha_2, \mathbf{z})^T\mathbf{w}_2, \tag{B6}$$

$$0 = \mathbf{w}_2^T\mathbf{w}_2 - 1, \tag{B7}$$

$$0 = \nabla_{\alpha_2}\mathbf{f}_P(\mathbf{s}_2, \alpha_2, \mathbf{z})^T\mathbf{w}_2, \tag{B8}$$

and

$$0 = 1 - \sum_{k=1}^{C} z_k. \tag{B9}$$

In total, Eqs. B1–B9 consists of $8C + 17$ equations and $9C + 14$ unknown variables. For a ternary mixture, the number of equations and the number of variables is identical and, therefore, $\mathbf{z}$ can be calculated using a solver for a set of nonlinear equations. Starting with a suitable initial guess using the information of the previously calculated pitchfork branches, the point of intersection of the two PDB is found at $\mathbf{z}^{(3)} = (0.62350592, 0.28412722, 0.09236684)$. Note that the lower pitchfork bifurcation in Figure B1 is only found if Eqs. B1–B9 are solved with high accuracy because the pinch map is extremely sensitive to perturbations in $\mathbf{z}^{(3)}$. Furthermore, a very good initial guess is required due to the high degree of nonlinearity in the set of equations. For the ternary example shown here, visual inspection of the point of intersection in Figure 4 was used to determine the points on the two PDB providing the initial guess.

*Manuscript received July 30, 2007, revision received May 25, 2010, and final revision received July 10, 2010.*